Simulation of a control system for the accident-free flight of three UAVs in the V formation in a heterogeneous environment

Altynbek Sh. Toleu[1], Aina Zh. Zakarina[1]
[1] Department of System Analysis and Management, L.N. Gumilyov Eurasian National University

ABSTRACT

Modern methods of creating groups of unmanned aerial vehicles (UAVs) require the use of complex (generalised) criteria, introduced mathematical models in the process of optimising the parameters of the UAV components. Such models should simulate the operation of an unmanned aerial vehicle when performing its task. The study considers strategies for diverging dangerously approaching UAVs using areas of dangerous courses and speeds. First, procedures were performed to establish the dangerous course areas of one UAV and the speeds of the second UAV, taking into account their ratio of speeds and dynamics. The areas for the case of UAV with insignificant transients of changes in courses and speeds, the duration of which can be neglected, is provided. In addition, procedures of the establishment of areas of dangerous courses of one UAV and the speeds of the second UAV with significant inertia are considered. Methods of the establishment of areas in the event of a decrease in the speed of the second UAV by active or passive braking are developed. Examples of choosing a safe manoeuvre in a situation of dangerous convergence of two UAVs are given. A more complex situation of approaching two UAVs in the presence of an interfering third UAV is also considered, and a method for choosing a safe manoeuvre is proposed, taking into account the interfering third UAV. Moreover, for such a situation, two alternative procedures for choosing a safe manoeuvre are proposed. The result of solving this problem was a method for establishing the area of dangerous courses and speeds of UAVs, taking into account the inertia-braking characteristics when determining a safe joint divergence manoeuvre taking into account the presence of a third UAV that provides interference.

Keywords:	Convergence, Divergence, Course, Distance, Movement

Corresponding Author:

Altynbek Sh. Toleu
Department of System Analysis and Management
L.N. Gumilyov Eurasian National University
010008, 2 Satpayev Str., Nur-Sultan, Republic of Kazakhstan
E-mail: toleu6566@nanyang-uni.com

1. Introduction

The experience of an autonomous adaptive system based on a swarm of 103 Perdix drones launched from three Boeing F/A-18E/F "parent aircraft" is taken into account when modelling the decentralised behaviour of UAVs in the V formation. Perdix micro-drones are not pre-programmed, they are a collective organism, sharing one distributed brain for making decisions and adapting to each other. This is how swarms of insects act in nature. Given the size of the flock (fleet), it is impossible to control drones from a single coordination centre (CC) individually. Since each Perdix communicates and cooperates with all other devices, the swarm does not have a leader and can smoothly adapt to any changes in the team [1]. But the swarm receives centralised general-purpose commands from a human operator, after which it executes them in an optimal way. A generalised model of interaction between a group of drones is shown in Figure 1, according to which UAVs communicate with each other. In some cases, global positioning or central commands are sent from the CC, but the flock should still be able to complete the task when communication with the CC is blocked [2].
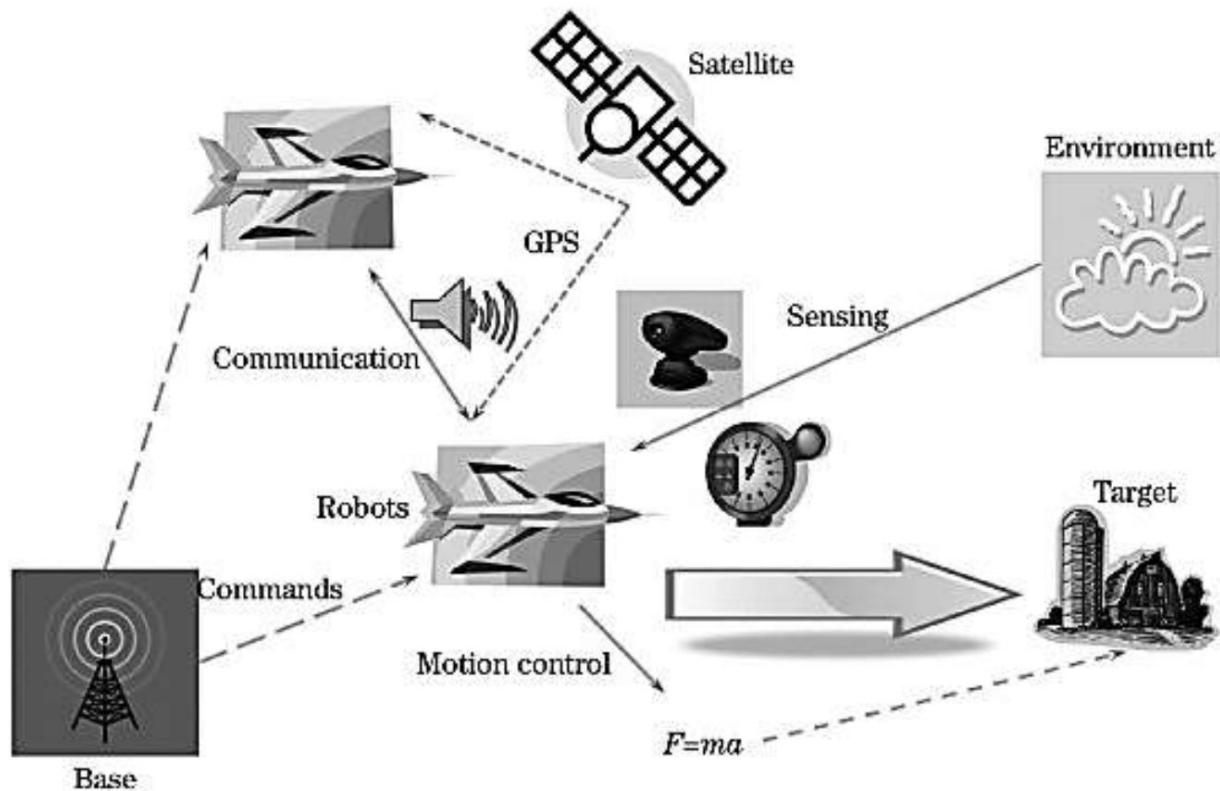
Figure 1. General model of a group of drones

In most research papers, groups of UAVs are classified as "swarms of drones", given their collective behaviour. But, taking into account the current trends in the development of industries in which UAVs are used, it is advisable to divide the flock into sub-swarms, given that different UAVs perform different tasks [3]. Objects that should perform the same (related) tasks – for example, measurements of weather data, it makes sense to generalise along the hierarchy into a "sub-swarm", all sub-swarms for a macro-task are combined into a "flock". Therefore, in order not to change the author's notation in the analysis, the author's term "swarm" is understood in the literature review as an enlarged group of UAVs (drones), which is not divided into "sub-swarms", which will already be called a "flock" in the subsequent (research) sections. Information exchange is necessary when UAVs will cooperate with each other, so the information exchange module is the main component for controlling the behaviour of the swarm. The main functions of the objects involved in such interaction are limited to peer-to-peer communication (peer-to-peer network). The interaction of pack objects in a heterogeneous network is the most common type of communication, and their behaviour can be described in the likeness of biological objects. Such a feedback mechanism would help optimise the behaviour of drones [4; 5].

There are three ways to exchange information in a pack: direct communication, communication through the environment and touch. More than one type of interaction can be used in one swarm, for example, each drone perceives the environment and communicates with its neighbours. Balch considered the influence of three types of communications in the swarm. This paper sets three tasks and compares the performance of modelling. Some researchers have also discussed the possibility of the swarm to interact without communication. However, communication and sensing can actually increase the effectiveness of the swarm for most cases. Direct communication is similar to the communication of objects (nodes) of a wireless network and also consists of two types: peer-to-peer network and broadcast. As a result of the development of mobile devices, it is possible to immediately adopt several existing technologies using IEEE (Institute of Electrical and Electronics Engineers) 802.11 b, a wireless LAN standard based on wireless data transmission in the 2.4 GHz band, bluetooth, and other wireless communication standards. However, wireless sensors cost almost half of the total UAV price [6; 7]. Another disadvantage of such a scheme is that the required bandwidth of the communication channel will increase exponentially with the growth of the swarm population. Thus, direct communication in swarms or flocks should be limited, for example, by a national regulator or a company that owns drones and integrates them into the national air system (Figure 2).
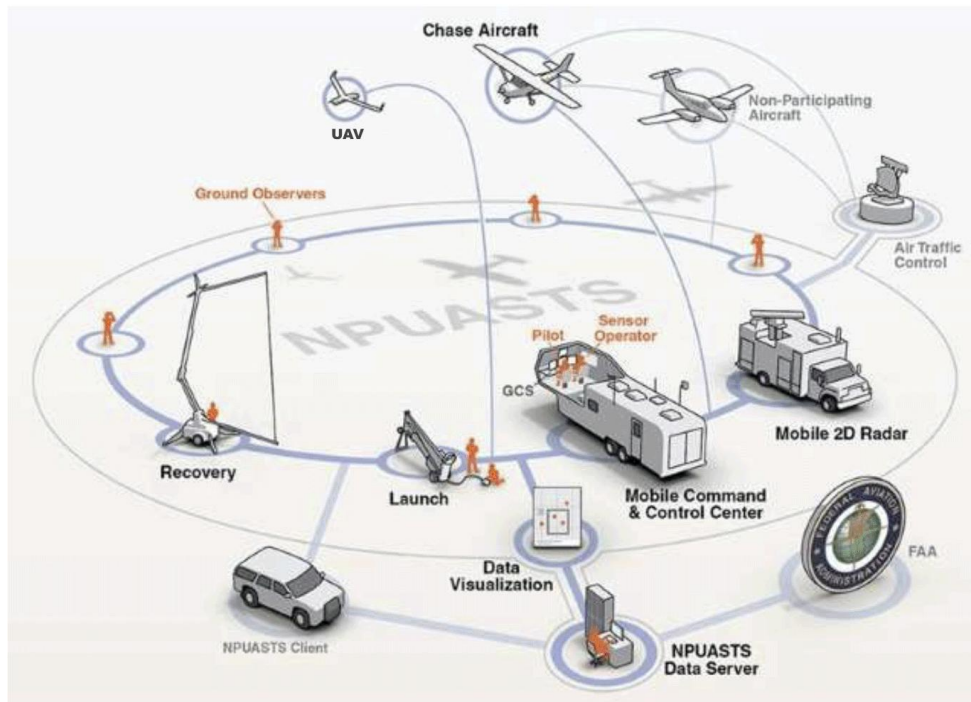
Figure 2. General infrastructure of the group of UAVs, implemented by the North Dakota Test Center for Unmanned Systems, which cooperates with NASA (National Aeronautics and Space Administration)

Communication, navigation and surveillance techniques are crucial to ensure that drones are under the constant control of the flock operator.

2. Theoretical overview

Although several existing wireless technologies are available, remote monitoring and control protocols and topologies that are based on group robotics remain undisclosed. Existing computer networks are designed for data processing and information exchange between nodes in the conditions of information adaptation of the data transmission system to the parameters of the communication channel [8; 9]. It is necessary to take into account not only the data transfer rate, but also such channel parameters as its asymmetry and signal strength. Communication in the drone group makes full use of sensing and signals to improve the overall behaviour of drones and the dynamic topology of remote monitoring and control. The environment can act as an intermediary for the interaction of drones. Drones can leave their tracks by removing "markers" in the environment after a certain action to inform other UAVs that can consider "order" without direct communication between other objects to the swarm. Thus, further actions, as a rule, are strengthened and rely on each other, which leads to the spontaneous appearance of activity at the swarm level. The swarm mimics the behaviour of ants or bees and interacts with the help of "virtual pheromones". Such an interactive scheme avoids an exponential increase in the number of connections between UAVs, but has some restrictions on the environment to support "virtual pheromones".

Drones can sense other UAVs and objects in the environment nearby thanks to the use of onboard sensors that can distinguish between UAVs and other environmental objects. UAVs read objects or targets in the environment and perform certain actions, such as avoiding mechanical obstacles, target search. The main problem of this scheme is how to integrate all sensors into the swarm effectively for cooperation [10]. The researchers investigated how to control and coordinate a group of autonomous vehicles, considered as agents with sensors, in an adaptive, distributed and asynchronous way. The main difference between communication and probing is whether people actively send a message or accept a message passively. While more accurate communication requires more sophisticated hardware and synchronisation, bandwidth, energy and time will grow very quickly along with the swarm population [11]. The cooperative model of a robotic group should try to simplify the way of communication and use probing as much as possible without communication. In some tasks, UAVs within a sub-swarm can exchange all information only with the help of sensors [12].

The distribution of tasks and training in this case is quite important for a swarm of UAVs. The task of decomposition and assignment can significantly increase the efficiency of particularly complex tasks. The

costs and benefits of different types of division tasks are compared [13; 14]. Training is also useful, since the control system parameters are difficult to update. With the help of self-adaptive training and optimisation methods, the swarm shows better adaptability in various environments. The problem of using various training methods in the swarm and their performance was compared on the simulator. An evolutionary neural network for the development of swarm management is used in the problem of reviewing the swarm structure. Security issues and technical factors that may prevent the drone from completing the task are subject to a detailed analysis:

− temperature of more than +40°C in summer and -20°C in winter (in which computer, mechanical and measuring equipment is inoperable);

− high wind speed (and sometimes sandstorms), which is able to change the course of the drone;

− a high degree of electromagnetic radiation, at which the UAV becomes uncontrollable, and the like [15; 16].

In addition to solving the issues of managing such single drones (fleet), it is necessary to pay attention to such issues as the use of different biometric data of recipients (fingerprints, eye recognition, etc.) by the security system to protect drones and their cargo. It is also necessary to make a decision (create an algorithm for the behaviour of the drone), what actions the UAV should perform with the contents of the portable container (memory module) in case of capture of the drone by unauthorised persons: launch the mechanism for destroying the container, defeat the invader. Modelling is used in many areas of research to better understand the internal structure of the system. The simulation helps the swarm, since the swarm must scale to several hundred and thousands of UAVs. Time and money are limited for such large-scale experiments, experiments can only be performed with single drones. Taking into account the characteristics of a group of drones, modelling methods are divided into four types: sensor-based, microscopic modelling, macroscopic modelling, and intelligence-based modelling [17].

In the first case, the sensors and devices of the UAV are modelled as the main components of the system together with the objects in the environment. Then the interactions between the UAVs are modelled as realistic and simple as possible. This modelling method is the most popular and the oldest used for experiments with robotic systems [18]. Previous studies using sensor-based modelling methods did not take into account real physical limitations, but now researchers have introduced real physical laws into the models. In microscopic modelling, UAVs and interactions are modelled as finite automata. The behaviour of each UAV is defined as a certain number of states, and the data transmission conditions are based on input data from the telecommunications system and sensors. Since the model is based on the behaviour of each UAV, the simulation must be run several times to get the average result of the swarm behaviour [19]. In most studies, the probable microscopic model has been used since the noise was modelled as a probability in the model. In the probable microscopic model, probabilities are estimated depending on experiments with real UAVs, and the model repeats this probability in the simulation to predict the behaviour of the swarm [20].

Macroscopic modelling is a modelling method that is the opposite of microscopic modelling. In macroscopic modelling, the state of the system is the average number of UAVs in a certain period of time. The main difference between microscopic and macroscopic modelling is the level of detail of the models [21]. The microscopic model is used for modelling at the individual level and at the group level, while the macroscopic model simulates behaviour at the swarm level. The microscopic model iterates over the behaviour of the swarm, and the macroscopic model can immediately give out the final state of the swarm. Thus, a macroscopic model can have a global view of the swarm, while a microscopic model can show details of the swarm behaviour [22]. Macroscopic probabilistic models are also widely used by researchers. Macroscopic modelling is applied to solve the problem of expanding from a basic model that contains only two states to a model with all states. The microscopic, macroscopic and sensor-based models are also compared and the disadvantages of the macroscopic model are described [23].

General schemes from intelligent swarm algorithms have been introduced into the robotics swarm in many studies. Since UAVs use the same or similar schemes with algorithms, models and other methods can also be used for swarms and flocks of UAVs. The most commonly used algorithm based on intelligence is the particle swarm method (PSM), which simulates the process of bird crowding. This is a numerical optimisation method, for which you do not need to know the exact gradient of the optimised function. Many successful swarm models have been created, taking into account the behaviour of ant colonies. These approaches provide effective heuristic algorithms for searching in a dynamic environment and for routing. There are still many problems when a group of drones with the intelligence of a swarm is presented. The schemes in these algorithms consider the most global interactions and introduce a large number of random moves for more unpredictable results. However, these operations would not be available for UAV sub-swarms, given the

specific nature of their tasks. Therefore, it is necessary to develop algorithms for the behaviour of individual sub-swarms, taking into account the uniqueness, scalability and flexibility of the tasks performed by them as part of the flock. Most of the provisions considered can also be extended to UAVs that move not only in the air environment. The basis of the behaviour of swarm members includes functions equipped with a control module (autopilot). Then the swarm objects can rely less on direct communication with each other.

Swarm can improve performance with less information exchange and high scalability. UAVs in a complex swarm system can have additional functions, including decomposition tasks, task distribution, adaptive learning, etc. UAVs using these functions in the hardware can simplify the structure of the motion algorithm to create a more complex physical design of drones. UAVs can perform similar functions with carefully designed cooperative algorithms. The implementation of such functions in hardware or software depends on the physical design of the UAV, controllers and sensors, and the best use of their computer components [24].

To develop further methods and algorithms for the creation and operation of sub-swarms as part of a UAV flock, it is necessary to formulate requirements for the availability of electronic components and software functions that are implemented by manufacturing companies on board the UAV. The main criteria for autopilot can be grouped according to a number of requirements. Obligatory:

1. The Return-to-Home (RTH) function, which would save computing power for returning to the start point at a certain level of battery discharge.
2. The "Cruise control" function for holding the flight altitude and course of the flight.
3. The "On Screen Display" (OSD) function, which displays the current coordinates and other flight parameters of the drone over the image from the camera.
4. Voltage readings from all batteries, which adjusts the time of the task by the drone depending on the residual voltage.
5. Absolute speed readings, which allows planning the size of the area for the survey.
6. Altitude readings (the presence of an altimeter on board), which allows taking into account the features of the terrain when laying the route.
7. Indications of the distance to the take-off point.
8. A compass to ensure the flight path in accordance with the laid theoretical route.
9. GPS (Global Positioning System) – a tracker for accurately determining the location of UAVs [25; 26].

Additional:

1. Temperature readings overboard, which allows diagnosing the critical use of the UAV in accordance with the parameters of the electronic equipment of the drone (within -20°C up to +40°C).
2. Relative speed readings, which allow developing algorithms for the operation of the flock in the absence of GPS coordinates.
3. Perimeter control functions, which would save computing power for returning to the starting point when crossing the border.
4. Stabilisation at relatively strong vibrations (during turns and at speeds of more than 90 km/h), which would save computing power to compensate for the "jelly effect" on images.

Necessary for the implementation of a controlled flight:

1. Transmission of coordinates in real time (with the display of the drone's position on the Google or Apple map).
2. The ability to connect an antenna to increase the flight range beyond the line of sight of the operator (more than 5 km) [27; 28].

Based on the technical characteristics of the available hardware solutions, when choosing UAV components, special attention should be paid to the choice of an autopilot, which should be equipped with a set of necessary sensors, be able to set flight points and change the route in flight, have an open-source software code and an open data exchange protocol, support for installation on various types of UAVs [29]. Preference in the choice of UAV autopilots is given to criteria that ensure the ability to function as part of a flock in complex non-deterministic conditions, namely: using Google services, controlling several drones simultaneously, choosing route points on the map, communication during flight [30]. Despite the constant additions to the functionality of drones, it is advisable to expand existing open-source developments by creating your own software for implementing additional services in the operation of a UAV flock.

3. Materials and methods

This section is devoted to solving an auxiliary task – determining a safe joint divergence manoeuvre of UAVs, taking into account their inertial characteristics. Taking into account the inertia of the first UAV turn and the

inertia-braking characteristics of another UAV when forming the boundaries of the region Ω_{KVf} assumes for each course K_{1y} of the first UAV to determine the braking speed of another UAV V_{2y}, at which the UAVs will disperse at the distance of the shortest approach D_{min} equal to the maximum permissible distance d_d. When calculating the braking speed of another UAV, it is assumed that its speed will decrease to the value V_{2y}, and then pass at this speed until the moment of the shortest approach, after which the other UAV increases the speed to the initial value. It is assumed that the manoeuvres of both UAVs begin at zero time. In general, the way to determine each point (K_{1y}, V_{2y}) limit of the domain Ω_{KVf} is as follows. The moment of the end of the rotation t_{yk} of the first UAV and the increase in its coordinates per hour of rotation is determined, taking into account the dynamic model of rotational motion. At this point in time, the current values of the UAV coordinates, the bearing and the distance between the UAVs are determined. To determine the increase in the coordinates of another UAV, its speed $V_{2t}(t_{yk})$ at the time of the hour t_{yk} is determined, and then the average speed:

$$V_{2m} = V_2 + [V_{2t}(t_{yk}) - V_2]/2 \tag{1}$$

and the changes in distance travelled:

$$S_{2m} = V_{2m}t_{yk}. \tag{2}$$

The relative course and distance of the shortest approach are determined by the values K_{1y}, V_1, K_2 and $V_{2t}(t_{yk})$. If it is less than the maximum permissible distance, then the speed value of the other UAV is reduced to the value:

$$V_{2y} = V_{2t}(t_{yk}) - 0.1, \tag{3}$$

for which the duration of the transition process, the distance travelled, the current coordinate values, bearing, distance, relative course and the distance of the shortest approach D_{min} are determined. The obtained distance of the shortest approach is compared with the maximum permissible distance d_d. If $D_{min} < d_d$, then the value of V_{2y} decreases again by 0.1 nodes and there is d_{min}, which is compared with d_d. The speed reduction V_{2y} in increments of 0.1 nodes is carried out until the equality D_{min} is reached $= d_d$. In the case when for all $V_{2y} \geq 0$ the specified equality is not achieved at all, it is impossible to perform a divergence manoeuvre by reducing the speed of another UAV. Therefore, to check the possibility of a safe stop with this manoeuvre, it is necessary to determine the distance of the shortest approach for a complete stop of another UAV. Next, the study considers the features of the establishment of the limits of the area Ω_{KVf} during the active and passive braking of another UAV during the divergence manoeuvre. For each of the evasion courses of the first UAV to the right, which belongs to the interval $[K_1 + 30, K_1 + 70]$, that is:

$$K_{1y}^{(s)} \in [K_1 + 30, K_1 + 70] \tag{4}$$

the possibility of a safe stop is determined by stopping another UAV by active or passive braking. To do this, it is decided that the braking of another UAV begins at the zero moment of time, and the beginning of the first turn of the UAV on the evasion course $K_{1y}^{(s)}$.

4. Results and discussion

Regardless of the braking mode of another UAV, the time interval for turning the first UAV and the increase in its coordinates per hour of rotation is estimated using a dynamic model of rotational motion. In the first approximation, the study uses the UAV rotation model with a constant angular velocity:

$$\tau_1 = \Delta K / a_\omega \tag{5}$$

where: a_ω – angular velocity of rotation; ΔK – increase in the course of the UAV, and:

$$\Delta K = K_{1y}^{(s)} - K_1. \tag{6}$$

The increase in the coordinates Δx_o and Δy_o of the first UAV per hour of manoeuvring τ_1 is determined by the following equations:

$$\Delta x_o = \frac{V_o}{a_\omega}\left(\cos K_1 - \cos K_{1y}^{(s)}\right) \tag{7}$$

$$\Delta y_o = \frac{V_o}{a_\omega}\left(\sin K_{1y}^{(s)} - \sin K_1\right) \tag{8}$$

In the case of using complex and adequate dynamic models of the rotational movement of the UAV, two phases of UAV rotation should be taken into account, the duration of which is Δt_k and Δt. The change in the course of the UAV K under the action of the steering in the second dynamic model of the rotational motion of the UAV is described by an inhomogeneous linear differential equation, which has the form:

$$T_1\ddot{K} + \dot{K} = k_\omega \beta_k \tag{9}$$

where: T_1 – time constant that takes into account the inertial properties of the UAV.

To calculate the time intervals Δt_k and Δt, it is necessary to create a system of k equations, which in general forms the requirements for turning on the problem of course increment ΔK, and reducing the angular velocity to zero at the time of entering a new course:

$$\Delta t_k = T_1[1 - exp(-\Delta t_k/T_1)] + \Delta t - T_1[2 - exp(-\Delta t_k/T_1)][1 - exp(-\Delta t/T_1)] + \Delta K/a_\omega \quad (10)$$

$$\Delta t = T_1 ln[2 - exp(-\Delta t_k/T_1)] \quad (11)$$

The calculation Δt_k and Δt is carried out by the method of simple iterations with an initial approximation:

$$\Delta t_k = \Delta K/a_\omega. \quad (12)$$

The last equation obtained allows relating the variable durations Δt_k and Δt, which ensures the iterative calculation of the values of each of the UAV rotation phases, and the duration of the turn τ from one given UAV course to another. To calculate the corrections to the moments of its rotation, taking into account the inertia of the UAV, it is necessary to calculate the increase in the coordinates Δx_o and the Δy_o operating UAV per hour of rotation τ. Thus:

$$\Delta x_0 = \int_0^{\Delta tk} V_0 \sin[K_0 + K]dt + \int_0^{\Delta t} V_0 \sin[K_0 + K(\Delta t_k) + \tilde{K}]dt \quad (13)$$

$$\Delta y_0 = \int_0^{\Delta tk} V_o \cos[K_o + K]dt + \int_0^{\Delta t} V_o \cos[K_o + (\Delta t_k) + \tilde{K}]dt \quad (14)$$

Attention is drawn to the fact that certain integrals included in the equations for Δx_o and Δy_o are not expressed in elementary functions and their values are found by numerical methods, for example, the trapezoid method is used or the Simpson method, which gives more accurate results (Skatkov et al., 2020). The third dynamic model of the UAV K course change during its rotation is described by an inhomogeneous third-order linear differential equation with constant coefficients, which has the following form:

$$T_1 T_2 \dddot{K} + (T_1 + T_2)\ddot{K} + \dot{K} = K_\omega \beta_k \quad (15)$$

where: T_1 and T_2 – time constants that characterise the inertial properties of the UAV.

The duration of the first Δt_k and the second Δt phase of the UAV rotation are found by the method of simple iterations from the system of equations:

$$\Delta t_k = \Delta t + \{T_1^2[1 - exp(-\Delta t_k/T_1)] - T_2^2[1 - exp(-\Delta t_k/T_2)]\}/(T_1 - T_2) -$$
$$-\{2 - [T_1 exp(-t_k/T_1) - T_2 exp(-\Delta t_k/T_2)]/(T_1 - T_2)\} \times \quad (16)$$
$$\times \{T_1^2[1 - exp(-\Delta t/T_1)] - T_2^2[1 - exp(-\Delta t/T_2)]\}/(T_1 - T_2) + \Delta K/a_\omega$$

$$\Delta t = -T_1 ln\{(T_2/T_1)exp(-\Delta t/T_2) + [(T_1 - T_2)/T_1] \times \times \{2 - [T_1 exp(-\Delta t_k/T_1) - T_2 exp(-\Delta t_k/T_2)]/$$
$$(T_1 - T_2)\}^{-1}\}, \quad (17)$$

After determining the increase in the coordinates of the first UAV as a result of rotation, for the initial speed of another UAV V_2 and the braking mode (active or passive), the run-out of the UAV S and the time interval τ_2 before the UAV stops are calculated. The coordinates of the first X_1, Y_1 and the other X_2, Y_2 UAV at the time of stopping the other UAV take the value:

$$X_2 = S \sin K_2, Y_2 = S \cos K_2 \quad (18)$$
$$X_1 = D \sin \alpha - V_1 \tau_2 \sin K_1 - \Delta x_o \quad (19)$$
$$Y_1 = D \cos \alpha - V_1 \tau_2 \cos K_1 - \Delta y_o \quad (20)$$

where: α – initial bearing from the second UAV to the first; D – distance between the UAVs.

At the time of stopping the second UAV, the distance between the UAV Df is determined by the equation:

$$V_1 = D \cos \alpha - V_1 \tau_2 \cos K_1 - \Delta y_o \quad (21)$$

Comparing the resulting distance D_f with the maximum permissible approach distance D_d. If $D_f < D_d$, then the difference between stopping the second UAV is impossible, and the point of the border of the area Ω_{KVj} with the coordinates $\left(K_{1y}^{(s)} V_2\right)$ does not exist. Another $\left(D_f > d_d\right)$ is calculated by the distance of the shortest approach of the first UAV with another UAV that stopped, D_{minf}:

$$D_{minf} = \left|D_f \sin\left[\alpha_f - K_{1y}^{(s)}\right]\right| \quad (22)$$

where: α_f – bearing on the second UAV at the time of its stop.

If $D_{minf} > D >_d$, then there may be a discrepancy by reducing the speed of the second UAV to a certain value V_{2y}, at which the equality is fulfilled:

$$D_{minf}\left(V_{2y}\right) = D_d \quad (23)$$

The speed value V_{2y} is calculated by the method of successive approximations, in which the braking speed of the second UAV is assumed to be equal to:

$$V_{2y} = V_2 - 0.1 \quad (24)$$

i on each i-th calculation cycle. The duration of the transition process $\tau(V_{2y})$ and the distance travelled $S(V_{2y})$ during this time for active braking are calculated using the following equations given in the third chapter:

$$\tau(V_{2y}) = \frac{(1+k)m}{\sqrt{\mu P}}\left[arctg\left(\frac{\sqrt{\mu}}{\sqrt{P}}V_2\right) - arctg\left(\frac{\sqrt{\mu}}{\sqrt{P}}V_{2y}\right)\right] \tag{25}$$

$$S(V_{2y}) = \frac{(1+k)m}{2\mu}\ln\left|\frac{V_2^2 + \frac{P}{\mu}}{V_{2y}^2 + \frac{P}{\mu}}\right| \tag{26}$$

where: $(1 + k)$ m – weight of the second UAV with the attached weights of water; P – stop of its screw; µ – resistance coefficient.

In the case of passive braking, the equations of the previous section are used:

$$\tau(V_{2y}) = \frac{(1+k)m}{\mu V_2}\left(\frac{V_2}{V_{2y}} - 1\right) \tag{27}$$

$$S(V_{2y}) = \frac{(1+k)m}{2\mu}\ln\left|\frac{V_2^2}{V_{2y}^2}\right| \tag{28}$$

The calculation process continues until the equality is fair:

$$D_{minf}(V_{2y}) = D_d \tag{29}$$

Thus, the boundary points are calculated for all the evasion courses $K_{1y}^{(s)}$ of the first UAV:

$$K_{1y}^{(s)} \in [K_1 + 30, K_1 + 70]. \tag{30}$$

Similarly, the calculation of the boundary of the area Ω_{KVj} for the UAV evasion courses to the left is performed. To establish the area of Ω_{KVj} dangerous courses of one UAV and the speeds of the second UAV, taking into account the inertia-braking characteristics of the second UAV, a computer programme was developed that implements the proposed algorithm for calculating the boundary of the area. As an example, the situation of a dangerous approach of a UAV with the following parameters was considered: $\alpha = 130°$, D = 3 miles, $K_1 = 130°$, $V_1 = 22$ knots, $K_2 = 315°$, $V_2 = 18$ knots, $D_d = 1$ mile. The predicted value of the distance of the shortest approach is exactly $D_{min} = 0.1$ miles, which indicates a dangerous approach of the UAV.

For the given situation of a dangerous approach of the UAV, Figure 3 shows the area Ω_{KVj} when the speed of the second UAV is reduced by passive braking. The combination of the UAV divergence parameters $K_{1y}^{(s)}$ and V_{2y} at the boundary of the region provides the distance of the shortest approach $D_{minf} = 1$ mile. Figure 4 shows the selected UAV divergence strategy with parameters $K_{1y}^{(s)} = 163°$ and $V_{2y} = 15.6$ nodes (the point limits are shown by concentric circles), which provide the shortest divergence distance $D_{minf} = 1.01$ miles.
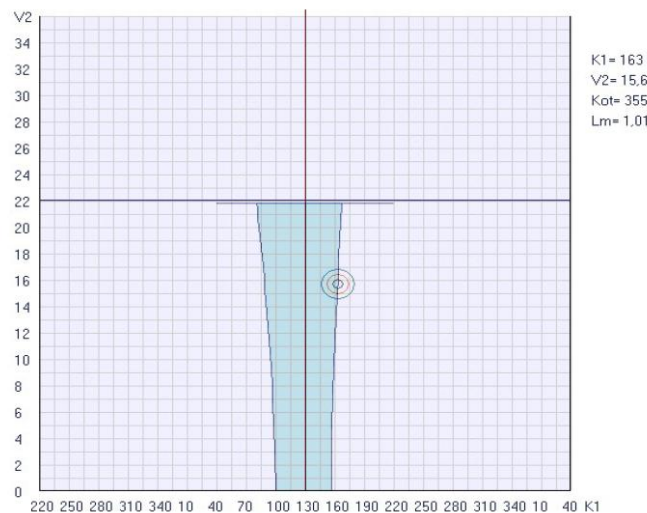
Figure 3. The area Ω_{KVj} under passive braking of the second UAV

When the first UAV dodged to the right by 33°, for a safe divergence of the second UAV, it was necessary to reduce the speed by passive braking by 6.4 knots. For the same situation of the dangerous approach, the programme formed an area Ω_{KVj} with active braking of the second UAV, shown in Figure 4. A Ω_{KVj} point corresponding to the parameters of the UAV divergence strategy is selected on the border of the region $K_{1y}^{(p)} = 85°$ and $V_{2y} = 18.4$ knots, at which the value of the distance of the shortest approach reaches the value $D_{minf} = 1.00$ mile, and the UAV divergence becomes safe. In this case, when the first UAV was dodging to the left by 35°, for a safe divergence of the second UAV, it was necessary to reduce the speed by active braking by only 3.6 knots.
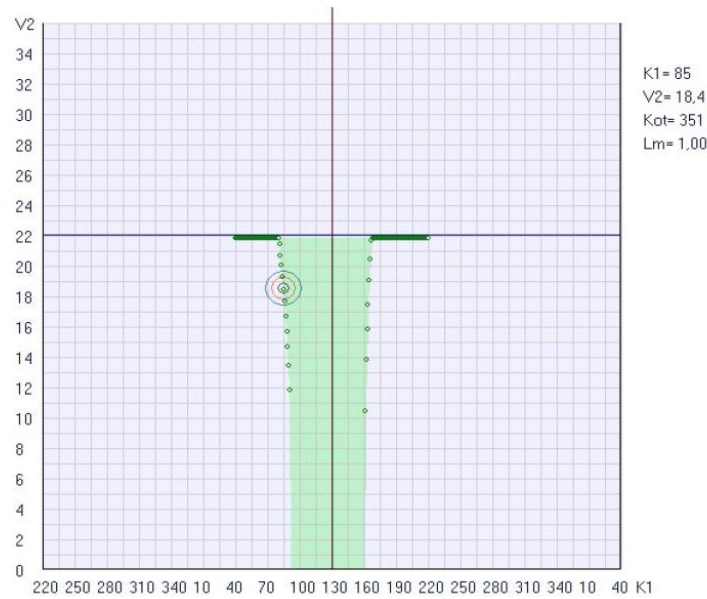
Figure 4. The area Ω_{KVj} under active braking of the second UAV

The result of the study was a method for forming the area of dangerous courses and speeds of the UAV, taking into account the inertial braking characteristics of the UAV when determining a safe joint divergence manoeuvre, which is the solution of the third auxiliary task. Usually, a procedure is obtained for selecting a safe joint divergence manoeuvre of the UAV area Ω_{KVj} with no interfering factors limiting the set of safe divergence manoeuvres. Next, the study considers the presence of a third UAV in the area of the proposed manoeuvring, which is not involved in the divergence process, but restricts the UAV divergence manoeuvre, since it can create a threat of dangerous rapprochement with one of them or with both UAVs. Such a third UAV will be called the interfering UAV. In the presence of an interfering UAV, the parameters of the divergence manoeuvre K_{1y} and V_{2y} for a safe difference must satisfy the condition of the advantage of the distances of the shortest approach between the UAVs over the maximum permissible distance of convergence, which is analytically expressed in this way:

$$\begin{cases} minD_{12}(K_{1y}, V_{2y}) \geq D_d \\ minD_{13}(K_{1y}) \geq d_d \\ minD_{23}(V_{2y}) \geq d_d \end{cases} \tag{31}$$

At the same time, the ratio of the predicted values of the time of the shortest approach of each pair of UAVs, which depend on the initial parameters of their movement, is very important. Admittedly, in the presence of an interfering UAV, three values of the time of the shortest approach should be considered: mint $_{12}$, mint $_{13}$ and mint $_{23}$. Most often, the situation of a dangerous approach to the interfering UAV is characterised by the ratio mint $_{12}$>mint>$_{13}$>mint>$_{23}$. In this case, for the manoeuvring first and second UAVs, an area of Ω_{KVj} unacceptable courses of the first UAV and the speeds of the second UAV should be formed, taking into account the braking mode, which takes into account the first equality of the system (31). After choosing a safe divergence manoeuvre, as points (K_{1y}, V_{2y}) the limits of the area Ω_{KVj}, it is necessary to calculate the value of the distance of the shortest approach $minD_{13}$ (K_{1y}) and $minD_{23}$ (V_{2y}), respectively, of the first and third, and the second and third UAV. The distance of the shortest approach $minD_{13}$ (K_{1y}) between the first and third UAV is determined based on the following considerations. Denoting the distance between the first and third UAV after the first UAV turn on the evasion course K_{1y} through D_{13k}, and the bearing is α_{13k}, then, given that both UAVs follow with unchanged motion parameters K_{1y}, V_1 and K_3, V_3, the shortest distance is determined by a known dependence:

$$minD_{13}(K_{1y}) = |D_{13k} \sin(K_{oyt13} - \alpha_{13k})| \tag{32}$$

where: K_{oty13} – relative exchange rate, which is calculated using the formula:

$$K_{oyt13} = arc \sin \left[\frac{(V_1 \sin K_{1y} - V_3 \sin K_3)}{[V_1^2 + V_3^2 - 2V_1 V_3 \cos(K_{1y} - K_3)]^{1/2}} \right] \qquad (33)$$

To determine the distance D_{13k} and the bearing α_{13k}, it is necessary to find the difference in coordinates ΔX_{13k} and ΔY_{13k} between the first and third UAV after the completion of the first UAV rotation, based on the initial values of the bearing α_n and the distance D_n. Thus:

$$\Delta X_{13k} = D_{13n} \sin \alpha_{13n} - \Delta x_o - V_3 \tau_1 \sin K_3 \qquad (34)$$

$$\Delta Y_{13k} = D_{13n} \cos \alpha_{13n} - \Delta y_o - V_3 \tau_1 \cos K_3 \qquad (35)$$

where: Δx_o and Δy_o – increment of the coordinates of the first UAV during the turn, which are determined by equations (5) and (8).

The values of the distance D_{13k} and the bearing are calculated using the equations:

$$D_{13k} = \sqrt{\Delta X_{13k}^2 + \Delta_{13k}^2} \qquad (36)$$

$$\alpha_{13k} = arc \sin \frac{\Delta X_{13k}}{D_{13k}} \qquad (37)$$

In turn, to determine the distance of the shortest approach $minD_{23}(V_{2y})$ between the second and third UAV, it is necessary to calculate the distance D_{23k} and the bearing α_{23k} between them at the time of the end of braking of the second UAV, when its speed of difference V_{2y} becomes unchanged. To do this, it is necessary to find the difference in coordinates ΔX_{23k} and ΔY_{23k} between the first and third UAVs at the specified time:

$$\Delta X_{23k} = D_{23n} \sin \alpha_{23n} - S \sin K_2 - V_3 \tau_b \sin K_3 \qquad (38)$$

$$\Delta Y_{23k} = D_{23n} \cos \alpha_{23n} - S \cos K_2 - V_3 \tau_b \cos K_3 \qquad (39)$$

where: α_{23n} and D_{23n} – initial bearing and the distance between the second and third UAV; τ_b and S – braking time of the second UAV and the distance travelled during this time, which are calculated using expressions (26) or (28), depending on the braking mode.

The distance D_{23k} and the bearing α_{23k} are calculated using the equations:

$$D_{23k} = \sqrt{\Delta X_{23k}^2 + \Delta Y_{23k}^2} \qquad (40)$$

$$\alpha_{23k} = arc \sin \frac{\Delta X_{23k}}{D_{23k}} \qquad (41)$$

The distance of the shortest approach $minD_{23}(V_{2y})$ between the second and third UAV is determined using the equation:

$$minD_{23}(Y_{2y}) = |D_{23k} \sin(K_{oty23} - \alpha_{23k})| \qquad (42)$$

where: K_{oty23} – relative exchange rate, which is calculated using the equation:

$$K_{oty23} = arc \sin \left[\frac{(V_{2y} \sin K_2 - V_3 \sin K_3)}{V_{2y}^2 + V_3^2 - 2V_{2y} V_3 \cos(K_2 - K_3)^{1/2}} \right] \qquad (43)$$

To assess the safety of the UAV manoeuvre differences in the presence of the third interfering UAV, a computer programme was developed, that, when choosing a manoeuvre divergence corresponding to a certain point in the border region Ω_{KVj}, also calculates distances $minD_{13}(K_{1y})$ and $minD_{23}(V_{2y})$, displays these values on the screen and compares with the maximum allowable distances of approach. As an example, Figure 6 shows the fourth standard situation of a dangerous UAV approach in the presence of a third interfering UAV, which is characterised by the parameters: $\alpha_{12} = 313°$, $D_{12} = 3$ miles, $K_1 = 339°$, $V_1 = 22$ knots, $K_2 = 102°$, $V_2 = 18$ nodes, $d_d = 1$ mile, $\alpha_{13} = 25°$, $D_{13} = 3$ miles, $K_3 = 224°$, $V_3 = 18$ knots. Reducing the speed of the second UAV is carried out by active braking. Figure 5 shows the area of Ω_{KVj} dangerous parameters of the course of one UAV and the speed of the second UAV for the given situation of convergence of three UAVs.
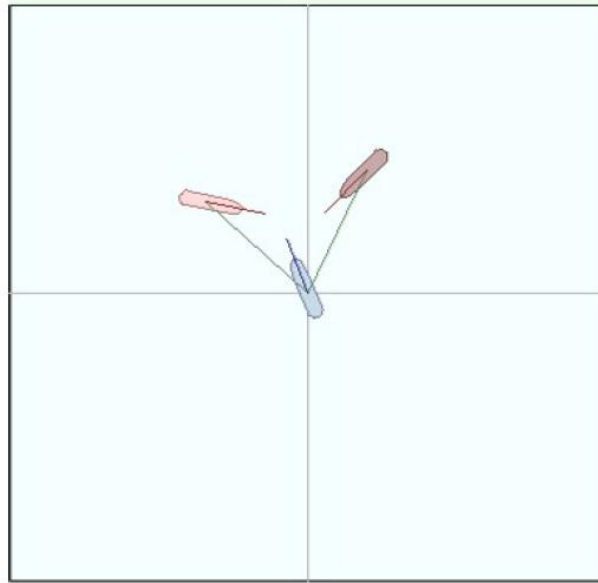
Figure 5. The fourth standard situation of the approach of three UAVs

The divergence manoeuvre corresponding to the boundary point of the region Ω_{KVj} with the parameters K_{1y} is selected = 4°, V_{2y} = 13.9 knots. Using the equations (32) and (42), the programme calculated the distances of the shortest approach $minD_{13}$ (K_{1y}) = 0.16 miles and $minD_{23}$ (V_{2y}) = 0.60 miles, which are less than the maximum permissible approach distance. This circumstance is shown in Figure 6 in the red colour of the information panels of the distances of the shortest approach.
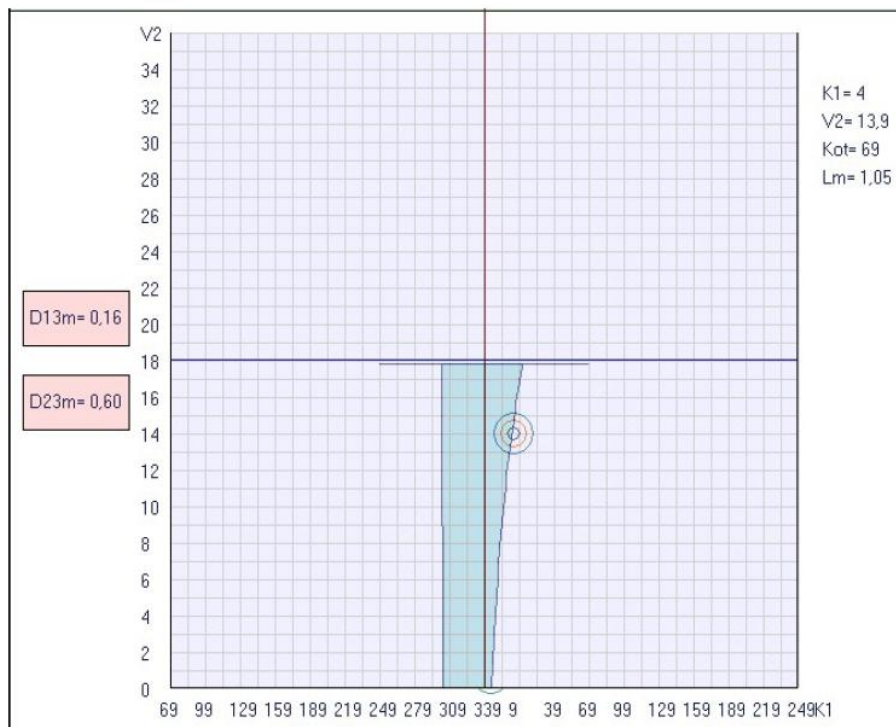
Figure 6. Choosing a divergence manoeuvre that is dangerous for the third UAV

In Figure 7, another divergence manoeuvre is selected with the parameters K_{1y} = 349° and V_{2y} = 4.5 knots. In this case, the distance of the shortest approach is $minD_{13}(K_{1y})$ = 0.59 miles and $minD_{23}(V_{2y})$ = 1.20 miles. Such a divergence manoeuvre is also unacceptable, since, at the permissible distances of the shortest approach $minD_{12}(K_{1y}, V_{2y})$ and $minD_{23}(V_{2y})$, the distance $minD_{13}(K_{1y})$ does not provide a safe divergence of the UAV.
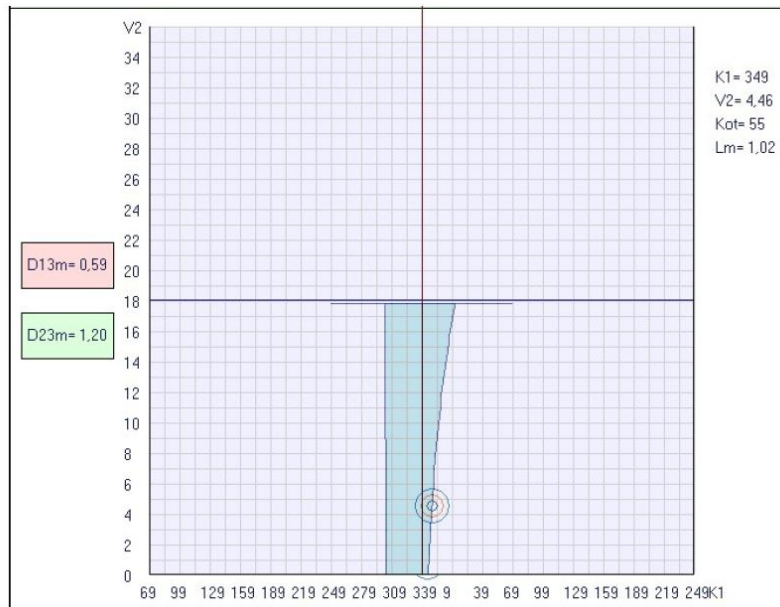
Figure 7. Manoeuvre with one dangerous approach

Therefore, another attempt was made to choose a safe manoeuvre, the results of which are shown in Figure 9. At the boundary of the area Ω_{KVj}, the selected manoeuvre with the parameters $K_{1y} = 296°$ and $V_{2y} = 7.15$ knots. As follows from Figure 8, the first and second UAVs diverge at a distance of 1.08 miles, the distances $minD_{13}$ (K_{1y}) = 2.04 miles and $minD_{23}$ (V_{2y}) = 1.03 miles exceed the maximum permissible approach distance. The selected manoeuvre is safe for all three UAVs, which confirms the green colour of the panels of the shortest approach distance.
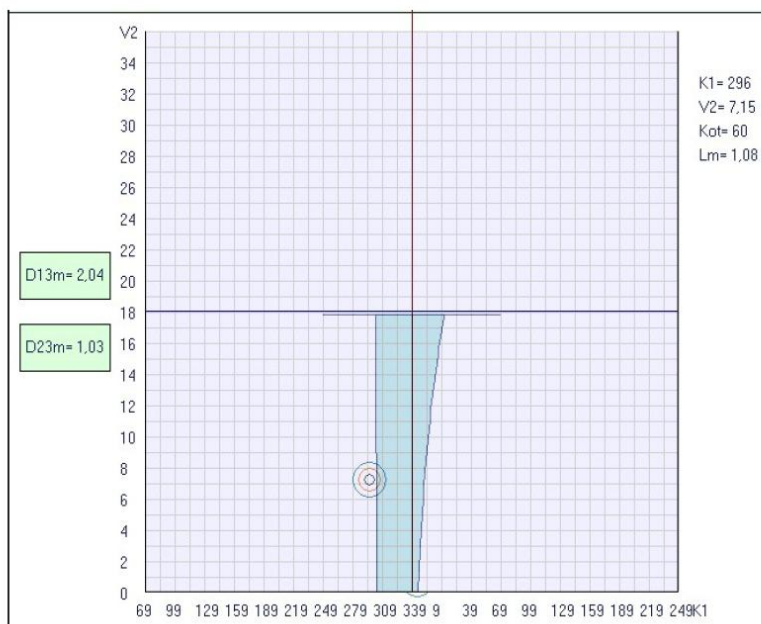
Figure 8. The divergence manoeuvre is safe for all UAVs

Next, the study considers the situation of the approach of three UAVs, when the second UAV uses passive braking to reduce the speed. This situation is the first standard situation of the approach of three UAVs (Figure 9). The selected situation is characterised by the following parameters: $\alpha_{12} = 144°$, $D_{12} = 3$ miles, $K_1 = 130°$, $V_1 = 22$ knots, $K_2 = 315°$, $V_2 = 18$ knots, $d_d = 1$ mile, $\alpha_{13} = 67°$, $D_{13} = 3$ miles, $K_3 = 225°$, $V_3 = 18$ knots. The speed reduction is performed by passive braking.
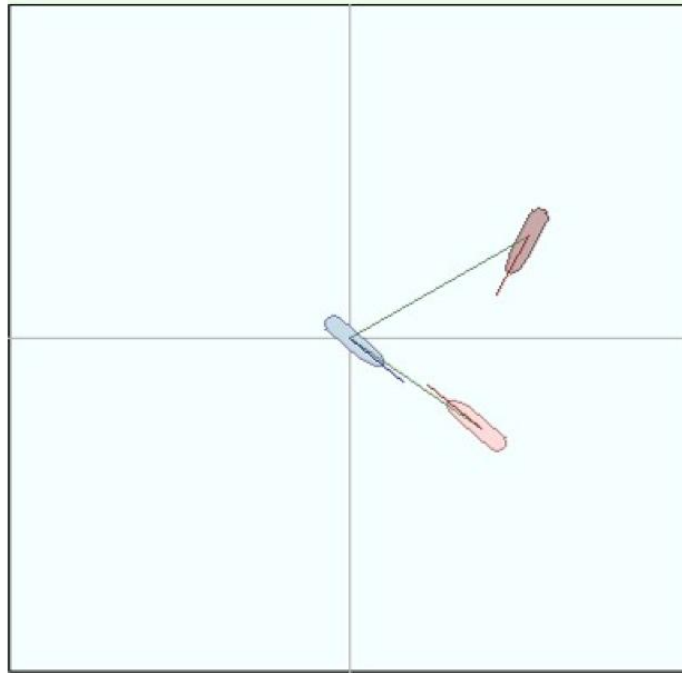
Figure 9. The first standard situation of the approach of three UAVs

Figure 10 shows the area Ω_{KVj} of the situation of convergence of three UAVs for passive braking and shows the choice of the divergence manoeuvre with the parameters $K_{1y} = 91°$ and $V_{2y} = 11.9$ knots. If the distances of the shortest approach $\min D_{12}(K_{1y}, V_{2y}) = 1.00$ miles and $\min D_{23}(V_{2y}) = 1.11$ miles are acceptable, then the distance of the shortest approach $\min D_{13}(K_{1y}) = 0.20$ does not provide a safe divergence of the first and third UAVs.

Figure 10. Manoeuvre with a dangerous approach of the first and third UAVs

When choosing a manoeuvre, there are discrepancies with the parameters $K_{1y} = 153°$ and $V_{2y} = 11$ nodes of the distance of the shortest approach of all UAVs, as follows from Figure 11, not less than the maximum permissible approach distance. Therefore, this manoeuvre is safe.

Figure 11. Safe divergence manoeuvre of three UAVs

As the above examples have shown, for the correct choice of a safe manoeuvre for the divergence of three UAVs, it is necessary to obtain conditions under which the distances of the shortest approaches $minD_{13}(K_{1y})$ and $minD_{23}(V_{2y})$ exceed the maximum permissible approach distance, depending on the movement parameters of the third interfering UAV. First, the study considers the convergence of the first and third UAVs after the turn of the first UAV, presented in Figure 12.
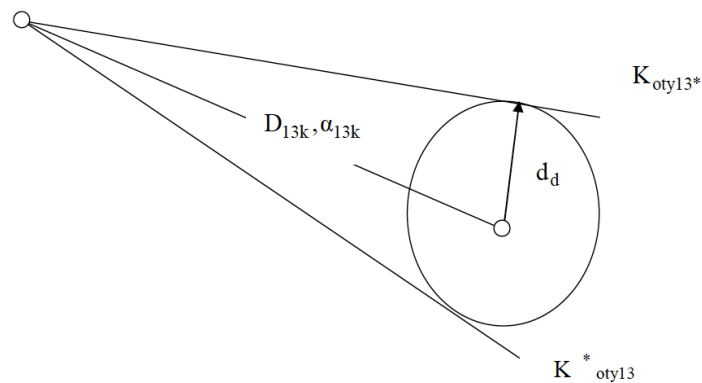
Figure 12. Marginal relative rates of K_{oty13*} and K_{oty13}^*

From Figure 13, it turns out that the relative courses K_{oty13} of the first and third UAVs are limited to the courses K_{oty13*} and K_{oty13}^*, at which the distance of the shortest approach $minD_{13}(K_{1y})$ is equal to the maximum permissible approach distance. For relative rates:

$$K_{oty13} \in [K_{oty13*}, K_{oty13}^*] \tag{44}$$

there is an inequality $minD_{13}(K_{1y}) < d_d$. Thus, for the relative courses K_{oty13*} and K_{oty13}^*, it is necessary to determine the corresponding limit courses K_{1y*}, which determine the possibilities of safe difference of the first and third UAVs. The paper shows the dependence of the true course of the UAV on the relative course, with the help of which obtain:

$$K_{1y*} = K_{oty13*} + arc\sin[p^{-1}\sin(K_3 - K_{oty13*})] \tag{44}$$

$$K_{1y}^* = K_{oty13}^* + arc\sin[p^{-1}\sin(K_3 - K_{oty13}^*)] \tag{45}$$

where: p = V1/V3:

$$K_{oty13*} = \alpha_{13k} - arc\sin\frac{d_d}{D_{13k}} \quad and \quad K_{oty13}^* = \alpha_{13k} + arc\sin\frac{d_d}{D_{13k}} \tag{47}$$

Thus, evasion course of the first UAV is chosen with the condition:

$$K_{1y} \notin \left[K_{1y^*}, K_{1y}^*\right] \tag{48}$$

Similarly, the maximum relative courses of the second and third UAVs are determined:

$$K_{oty23^*} = \alpha_{23k} - arc \sin\frac{d_d}{D_{23k}} \tag{48}$$

$$K_{oty23}^* = \alpha_{23k} + arc \sin\frac{d_d}{D_{23k}} \tag{49}$$

However, when approaching the second and third UAVs, it is necessary to find the speed limits of the second UAV. Therefore, it is necessary to find the dependence of the UAV speed on the relative course. As follows:

$$tgK_{ot} = \frac{\sin K_{ot}}{\cos K_{ot}} = \frac{V_1 \sin K_1 - V_2 \sin K_2}{V_1 \cos K_1 - V_2 \cos K_2} \tag{51}$$

the last equation:

$$(V_1 \sin K_1 - V_2 \sin K_2) \cos K_{ot} = (V_1 \cos K_1 - V_2 \cos K_2) \sin K_{ot} \tag{52}$$

or, grouping the components by UAV speeds:

$$V_2(\cos K_2 \sin K_{ot} - \sin K_2 \cos K_{ot}) = V_1(\cos K_1 \sin K_{ot} - \sin K_1 \cos K_{ot}) \tag{53}$$

The brackets of the last equation contain expressions of the sine of the difference between the two arguments. Thus:

$$V_2 \sin(K_{ot} - K_2) = V_1 \sin(K_{ot} - K_1) \tag{54}$$

From the last expression, it turns out:

$$V_2 = V_1 \frac{\sin(K_{ot} - K_1)}{\sin(K_{ot} - K_2)} \tag{55}$$

Therefore, taking into account the equation (50) for the maximum speeds at the approach of the second and third UAV:

$$V_{2y}^* = V_3 \frac{\sin\left(K_{oty23}^* - K_3\right)}{\sin\left(K_{oty23}^* - K_2\right)} \tag{55}$$

$$V_{2y^*} = V_3 \frac{\sin\left(K_{oty23^*} - K_3\right)}{\sin\left(K_{oty23^*} - K_2\right)} \tag{56}$$

For the fourth standard situation, an area was obtained Ω_{KVj} when the second UAV was actively braking, which is shown in Figure 13.
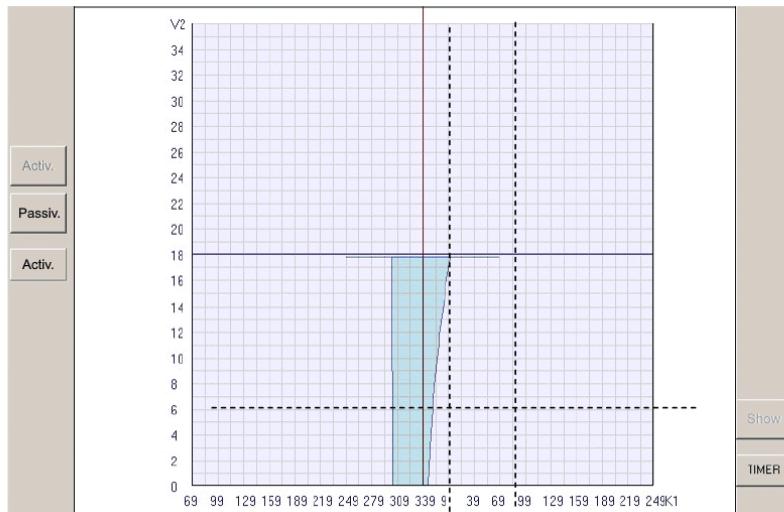
Figure 13. Limit courses and speeds for the fourth standard situation

Using the equation (50), the values of the limit courses $K_{1y^*} = 334°$ and $K_{1y}^* = 45°$ were calculated, which are shown by vertical lines. The values of the maximum speeds $K_{1y}^* = 7.5$ knots and $V_{2y^*} = 0$ are determined using the equations (57) and are shown by horizontal lines in Figure 14.

5.   Conclusions

The hardware basis of any UAV is a flight controller that collects data from sensors, controls stabilisation and position in space. Commands to the flight controller can be sent from the remote control or from the ground station. As a result, the engine speeds change, which allows the UAV to move in the air. The use of an on-

board mini-computer connected directly to the flight controller combines the advantages of manual remote control and a ground station, allows automating the flight and interacting with the outside world, using the measured environmental parameters for autonomous flight. Based on the analysis of the structures of network interaction of objects of heterogeneous networks, the advantages of using centralised control of the entire group of devices with a small number of UAVs are revealed.

With an increase in the number of UAVs in the group, the load on the communication channel between the coordination centre (operator) and each unmanned vehicle, and directly on the coordination centre, increases. Therefore, the further development is the construction of heterogeneous structures of computer networks with the development of swarm control methods for a flock of UAVs divided into sub-swarms. It is proved that the most promising is the development of methods and algorithms for redefining tasks and planning routes of UAVs, taking into account the aerodynamic properties of remote monitoring and control and achieving self-regulation of the network structure. The requirements for the availability of electronic components and software functions that must be implemented in the flight controller on board of an unmanned aerial vehicle are formulated. The expediency of using the Hopfield neural network for the establishment of routes for the movement of UAVs in limited spatial corridors is substantiated. Most solutions for UAVs are workable and effective for other types of unmanned vehicles that move in a different environment, not only in the air.

References

[1] D. A. Antonov, K. K. Veremeenko, M. V. Zharkov, R. Y. Zimin, I. M. Kuznetsov, and A. N. Pron'kin, "Fault-tolerant integrated navigation system for an unmanned apparatus using computer vision", *Journal of Computer and Systems Sciences International*, vol. 59, pp. 261-275, 2020.

[2] V. V. Borodin, A. M. Petrakov, V. A. Shevtsov, and T. Y. Shevgunov, "Multi-station access without acknowledgement in IoT networks", *Russian Aeronautics*, vol. 62, no. 3, pp. 522-526, 2019.

[3] A. V. Terleev, A. A. Khalturin, and V. A. Shpenst, "LoRaWAN gateway coverage evaluation for smart city applications", in: *Proceedings of the 3rd 2021 International Youth Conference on Radio Electronics, Electrical and Power Engineering, REEPE 2021, article number 9388004*. Moscow: Institute of Electrical and Electronics Engineers Inc, 2021.

[4] R. Roberts, M. Barajas, E. Rodriguez-Leal, and J. L. Gordillo, *Haptic feedback and visual servoing of teleoperated unmanned aerial vehicle for obstacle awareness and avoidance*, 2017. https://journals.sagepub.com/doi/pdf/10.1177/1729881417716365.

[5] Y. Song, Y. Liu, W. Xu, X. Yang, and R. Wang, "Research on the multiobjective optimization of microwave wireless power receiving in an unmanned aerial vehicle network", *Complexity*, vol. 2020, article number 8882528, 2020.

[6] I. O. Akimov, and V. V. Koryanov, "Numerical simulation of the motion of an unmanned aerial vehicle", *MATEC Web of Conferences*, vol. 221, article number 05003, 2018.

[7] L. Fu, L. Peizhi, and C. Weiyan, "Design of high voltage surge suppression circuit for unmanned ground vehicle computer system", in: *Proceedings of 2017 IEEE International Conference on Unmanned Systems (pp. 539-543)*. Piscataway: IEEE, 2018.

[8] A. Yu. Burova, and V. V. Kabakov, "Automatic control of working car engine vibrations using multi-stage discrete Fourier transformation". *Journal of Physics: Conference Series,* vol. 1679, no. 2, article number 022025.

[9] E. Lygouras, and A. Gasteratos, "A novel moving-base RTK-GPS-Based wearable apparatus for precise localization of humans in peril", *Microprocessors and Microsystems*, vol. 82, article number 103833, 2021.

[10] J. B. Wolf, E. Shelley, and D. Stralka, *Design of an engine air particle separator for unmanned aerial vehicle applications*. 2016. https://arc.aiaa.org/doi/10.2514/6.2016-0406.

[11] S. E. Tsybulevsky, I. M. Murakaev, P. E. Studnikov, and A. V. Ryapukhin, "Approaches to the clustering methodology in the rocket and space industry as a factor in the formation of a universal production model for the economic development in the space industry", *INCAS Bulletin*, vol. 11, pp. 213–220, 2019.

[12] A. V. Skatkov, D. V. Moiseev, and A. A. Bryukhovetskiy, *Model for vulnerabilities detection in unmanned vehicle interfaces based on artificial immune systems*. 2020. https://iopscience.iop.org/article/10.1088/1742-6596/1515/2/022043/pdf.

[13] Yu. A. Surkov, V. F. Ivanova, A. N. Pudov, E. P. Sheretov, B. I. Kolotilin, M. P. Safonov, S. P. Ovchinnikov, N. V. Veselkin, V. F. Samodurov, V. S. Gurov, R. Thoma, G. Lespaniol, and A. Osier, "Mass spectrometer of Vega-1 unmanned interplanetary station", *Instruments and Experimental Techniques New York*, vol. 32, pp. 921-925, 1990.

[14] S. Barnett, *Development of a tow capacity test device for small unmanned vehicles*. 2005. https://vtechworks.lib.vt.edu/bitstream/handle/10919/30968/Barnett_Thesis.pdf?sequence=1&isAllowed=y.

[15] S. V. Luniov, A. I. Zimych, P. F. Nazarchuk, V. T. Maslyuk, and I. G. Megela, "Specific features of electron scattering in uniaxially deformed n-Ge single crystals in the presence of radiation defects" *Radiation Effects and Defects in Solids*, vol. 171, no. 11-12, pp. 855-868, 2016.

[16] S. Yoshida, M. Tanomura, Y. Hama, T. Hirose, A. Suzuki, Y. Matsui, N. Sogo, and R. Sato, *Underwater wireless power transfer for non-fixed unmanned underwater vehicle in the ocean*, 2016. https://ieeexplore.ieee.org/document/7778668/authors#authors.

[17] E. A. Fedulova, A. O. Akulov, A. O. Rada, T. A. Alabina, and J. J. Savina, *Reducing environmental damage through the use of unmanned aerial vehicles as the best available technology*, 2018. https://iopscience.iop.org/article/10.1088/1755-1315/115/1/012012/pdf.

[18] O. Frånberg, M. Loncar, A. Larsson, H. Örnhagen, and M. Gennser, "A metabolic simulator for unmanned testing of breathing apparatuses in hyperbaric conditions", *Aviation, Space, and Environmental Medicine*, vol. 85, no. 11, pp. 1139-1144, 2014.

[19] X. Sun, "Research on power patrol system of small unmanned aerial vehicle based on BDS/GIS", *Technical Bulletin*, vol. 55, no. 7, pp. 747-752, 2017.

[20] Y. He, J. Wu, S. Shi, Z. Song, Q. Qiao, and C. Wang, "Wireless electricity transmission design of unmanned aerial vehicle charging systems", in: Q. Liang, W. Wang, X. Liu, Z. Na, M. Jia, B. Zhang (Eds.), *Communications, Signal Processing, and Systems* (pp. 762-768). Cham: Springer, 2020.

[21] M. I. Gordeeva, and Y. A. Knyazeva, "The structure and properties of laminated aluminum-glass reinforced plastics", *IOP Conference Series: Materials Science and Engineering,* vol. 889, no. 1, article number 012015.

[22] D. Kritskiy, S. Yashin, and S. Koba, "Unmanned aerial vehicle mass model peculiarities", in: S. Shkarlet, A. Morozov, A. Palagin (Eds.), *Mathematical Modeling and Simulation of Systems* (pp. 299-308). Cham: Springer. 2021.

[23] K. Kakutani, Y. Matsuda, T. Nonomura, Y. Takikawa, K. Osamura, and H. Toyoda, "Remote-controlled monitoring of flying pests with an electrostatic insect capturing apparatus carried by an unmanned aerial vehicle". *Agriculture*, 11(2), article number 176, 2021.

[24] A. Y. Burova, "Minimization of asymmetry of thrust of dual-flow turbojet engines of airliner in accordance with the results of system analysis of thrust parameters", *Asia Life Sciences*, vol. 2, pp. 629-643, 2019.

[25] T. Y. Shevgunov, Z. A. Vavilova, O. A. Guschina, and E. N. Efimov, "Heuristic global optimization algorithm for estimating a radio source location by a passive radar system", *TEM Journal*, vol. 9, no. 2, pp. 427-433, 2020.

[26] J. Wang, Y. Wu, Y. Yang, W. Gu, and J. Mo, *Analysis on sway of spilled oil recovery apparatus lifted up from unmanned surface vehicle,* 2014. https://ieeexplore.ieee.org/document/6964530.

[27] E. M. Dobychina, M. V. Snastin, E. N. Efimov, and T. Y. Shevgunov, "Unmanned aerial vehicle antenna measurement using anechoic chamber", *TEM Journal*, vol. 9, no. 4, pp. 1480- 1487, 2020.

[28] X. Li, K. Sun, and F. Li, "General optimal design of solar-powered unmanned aerial vehicle for priority considering propulsion system", *Chinese Journal of Aeronautics*, vol. 33, no. 8, pp. 2176-2188, 2020.

[29] T. Y. Shevgunov, and G. V. Malshakov, "Method of achieving interoperability of applied software based on the analysis of their data". in: *Conference Proceedings "2020 Systems of Signals Generating and Processing in the Field of on-Board Communications"* (article number 9078549). Moscow, Institute of Electrical and Electronics Engineers Inc, 2020.

[30] O. D. Dantsker, R. W. Deters, and M. Caccamo, *Propulsion system testing for a long-endurance solar-powered unmanned aircraft,* 2019. https://arc.aiaa.org/doi/10.2514/6.2019-3688.